Journal of Techniques, ISSN: 2708-8383, Vol. 5, No. 4, 2023, Pages 16-27
DOI: https://doi.org/10.51173/jt.v5i4.1005

JOURNAL OF TECHNIQUES

Journal homepage: http://journal.mtu.edu.iq

RESEARCH ARTICLE - ENGINEERING

A Hybrid Renewable Sources Implementation for a DC Microgrid with Flatness-Nonlinear Control to Achieve Efficient Energy Management Strategy

Furqan A. Abbas[1*], Adel A. Obed[1], Ammar Alhasiri[2], Salam J. Yaqoob[3]

[1]Electrical Engineering Technical College, Middle Technical University, Baghdad, Iraq

[2]Istanbul Gelisim University, İstanbul, Turkey

[3]University of Jaén, Jaén, Spain

[*] Corresponding author E-mail: Furqan.Aldhahir94@gmail.com

Article Info.

Article history:

Received
12 October 2022

Accepted
07 February 2023

Publishing
31 December 2023

Abstract

The significance of energy management using sustainable energy sources and the merits of DC in AC microgrids are due to less complexity, smaller size, and fewer conversion stages. In this paper, we propose a standard-islanded DC microgrid with photovoltaic (PV) and fuel cell (FC) primary sources and a supercapacitor (SC) storage unit. The proposed system provides high-quality energy supplied to the DC load under different levels of solar irradiation and changing loading situations. Taking into account the slow dynamic response of the FC, the SC provides transient periods under various conditions to maintain stability of the system. Because of the nonlinear system's behavior, differential flatness-based control has been applied mainly in nonlinear systems where the number of variables to the outputs is reduced with a robust control system established through inherited parameter reductions and equality constraints due to the system trajectories (x, u) is straightforwardly estimated from flat output trajectories y and their derivatives without any differential equation integration. The PI control is executed when the SC adjusts the DC bus voltage variation. Therefore, the objective is to provide management that ensures stable DC bus voltage and arranges power sharing between variable sources and power balance with a load. Flatness PI has been investigated and has proven effective in offering faster response without overshoot and greater robustness.

Publisher: Middle Technical University

Keywords: Differential Flatness; Energy Management System (EMS); Energy Storage System; Fuel Cell; Microgrid; Photovoltaic (PV).

1. Introduction

The world is moving toward excellent and adequate power sources such as renewables (photovoltaic, wind, biomass, fuel cells, etc.). Researchers are working on ways to combine several renewable energy sources because fossil fuels are running out, greenhouse gas emissions must be cut down, and there is a high demand for electricity.One of the most promising renewable energy generation technologies is the photovoltaic (PV) source [1]. Solar energy is one of these environmentally acceptable alternatives. Solar panels or central solar power technologies depend on thermal energy and can transform it directly into electricity [2]. Due to the various advancements, they have made (such as low emission of polluting gases, high efficiency, and flexible modular structure) [3]. Fuel cells (FCs) are among the most reliable sources for future energy supply and are regarded a powerful specific energy source. FCs are a very environmentally friendly source for microgrids due to their efficiency, dependability, and power density [4, 5]. A hybrid power system should include a minimum of one additional source (a storage device) to prevent voltage drops and supply the load during the trainset period. Therefore, it is recommended to apply a current control loop when using FC is advised to avoid overload and improve performance.The efficiency of supercapacitors (SCs) is higher than that of batteries (BAT) because the slow charging period of the charging current affects their efficiency (50% for the battery), unlike SCs, which are characterised by a rapid response with a high energy density (95% for SC) [6]. Furthermore, SCs must change quickly on the charge current (power) available. In contrast to batteries, SCs can withstand a large number of cycles of charge and discharge without degradation (virtually indefinite cycles). Consequently, SCs are more potent, last longer and have faster dynamic behavior than batteries [7].

Each source has its limitations. For example, FCs require hydrogen-rich fuel, solar energy is climate-dependent due to its sporadic output, and there is a difference between supply and demand that compromises the stability and dependability of the grid[8]. PV can comprise the microgrid with another source like wind or diesel generator [9-11]. It has been widely used for several purposes, including agriculture [12]. The operation of these various renewable energy sources in combination is more complex than the operation of them separately. Only one component is controlled in a system that includes only solar energy or FC. However, when they work together, each component has to be controlled individually. In addition to being controlled together, each component must adjust separately to make them work together so that they are operated accordingly. The solar panel cannot supply constant power when the solar energy level changes. Similarly, the FC will not work when

Nomenclature & Symbols

EMS	Energy Management System	$P_{PVo}, P_{FCo}, P_{SCo}$	Actual Power of PV, FC and SC
MG	Microgrid	P_{load}	Load Power
SoC	State of Charge	r_{PV}, r_{FC}, r_{SC}	Losses Converter of PV, FC and SC
DC	Direct Current	v_{PV}, v_{FC}, v_{SC}	Instantaneous Voltage of PV, FC and SC
AC	Alternating Current	i_{PV}, i_{FC}, i_{SC}	Instantaneous Current of PV, FC and SC
FC	Fuel Cell	y_{bus}	DC Bus Capcitive Energy
PI	Proportional Integral	P_{Gen}	Generation Power
SC	Supercapacitor	y_T	The Total Electromagnetic Energy
MPC	Model Predictive Control	P_{PV}, P_{FC}, P_{SC}	Reference Power of PV, FC and SC
PV	Photovoltic	$P_{SC,max}$	Maximum Limited Power of SC
MINC	Modified Incremental Conductance	K_p, K_1	Proportional Gain of PI Controller
MPPT	Maximum Power Point Tracking	K_i, K_2	Integral Gain of PI Controller
GWO	Gray Wolf Optimization	$P_{FC\,max}, P_{PV\,max}$	Maximum Generated Power of PV, FC
PEMFC	Polymer Electrolyzer Membrance Fuel Cell	G	Solar Irradiation
SOFC	Solid Axide Fuel cell	I_{scr}	Reverse Saturation Current
FLC	Fuzzy Logic Controller	k_i	Temperature Coefficient
BAT	Battery	T_c	Cell Temperature
UC	Ultra-Capacitors	T_{ref}	Refrence Temperature
I_o	Saturation Current	V_{oc}	Open Circuit Voltage
k	Boltzman Constant	I_{sc}	The Photocurrent
q	Electron Charge	n	Ideality Factor
V	Diode Voltage	P_{load}	Load Power
I_{ph}	Light Generated Current	V_{bus}	Bus Voltage
I_s	Saturation Current	i_{load}	Load Current
$\dot{y_{bus}}$	Derivative of DC Bus Energy	$C_{bus,} C_{sc}$	Capacitance of DC Bus and Supercapacitor
V_{sc}	Supercapacitor Voltage		

there is no fuel. If one of these sources generates less energy than the required amount, then the other source is managed to supply the remaining amount so that the load runs normally. The management system's goal is to make correct decisions that supply the load continuously and receive the required power at the rated voltage and power values [13]. It is well recognized that adding more distributed generators to a power grid can caused problems including increased voltage and instability [14]. These problems may damage some delicate electrical loads. Therefore, a robust management algorithm must address these issues and guarantee consistent DC bus voltage versus environmental changes (weather conditions or demand).

In this paper, an energy management strategy based on flatness-PI control has been implemented to ensure the stabilisation of the dc bus voltage and arrange power-sharing between PV, FC, and SC to achieve the power balance between generation and demand under different operation conditions for the islanded DC microgrid. Also, the effectiveness of the proposed strategy is confirmed by comparing it with another study.

The rest of the article shows the literature review in Section 2. and the main design aspects of system and methodology in Section 3. While Section 4 presents Result and discussion. Finally, the conclusions in Section 5.

2. Literature Review

Smart energy management using the fuzzy logic controller (FLC) algorithm to turn on and off the system supplying power to loads consisting of renewable energy resources is studied, where an EMS is required for sustainable energy supply for users because the performance of such sources varies depending on the time of day and season of the year [13]. An EMS of a grid-connected hybrid system combines PV, BAT, and a hydrogen chain (FC, electrolyzer, and hydrogen tank) depending on the Model Predictive Control (MPC) approach, which predicts the future output behaviour of the storage system handling the power balance between the electricity supplied by the hybrid plant and the demand [15]. The previous two studies did not achieve regulation of the DC bus voltage. A hybrid DC/AC MG consisting of PV and FC is presented, where the main aim is to improve the power quality of the MG using grey wolf optimization (GWO) based on the MPPT technique under MATLAB/Simulink. Furthermore, it ensures the most active power supply to the main grid [16]. In [17] a typical hybrid microgrid based on PV and FC where an equalized power flow can be achieved FLC-based voltage-frequency control (V/f) without power sharing between sources. While in [18] power sharing between BAT and SC energy storage devices is controlled by a variable structure based on sliding mode control (SMC) and PI to regulate the voltage of the DC bus and address the generation-demand difference. In [19] a standalone DCMG comprised of PV with primary (SC_1, SC_2) and BAT secondary storage systems based on an adaptive FLC in three different modes, considering power sharing between storage devices only and maximizing utilization of energy storage devices,adding complexity to the system. An EMS for a hybrid power system composed of FC, Ultra-Capacitors (UC), and BAT specified for electric vehicles depends on the incorporation of two control processes to demonstrate the efficiency of the proposed control strategy by balancing energy between sources to meet the load demand: FLC and differential flatness control have been used [20].

Finally, previous studies that covered the concept of MG and different energy management strategies did not focus on the various operating conditions affecting the system. Therefore, an energy management strategy at different angles with various control strategies will be achieved in this paper. Recently, these approaches have been applied to numerous nonlinear systems in a variety of engineering disciplines, including

control of cathode pressure and oxygen excess ratio of a PEMFC [21], reactive power and dc voltage tracking control of a three-phase voltage source converter [22], current control for three-phase three-wire boost converters[23], and control of robotics[24].

3. The Hybrid Scheme Construction

3.1. System structure

A microgrid has been planned to run in islanded mode. The implementation is checked by estimating different loads where the PV and FC represent the main energy sources to meet the requirement for power, while the SC provides the energy necessary to maintain the DC bus voltage through transient times. The suggested exemplary comprises five parallel, two series of PV strings, a FC, and a SC, that are connected to the DC bus across different DC/DC converters (380 V) to manage power sharing and maintain the DC bus voltage.

Fig. 1 illustrates the construction of the proposed system with different power electronic converters, demonstrating the parallel connection of all converters. Two-phase interleave boost converter regulate the FC stack and reduce input current and output voltage ripple, improving power quality[25, 26] . It is also used to regulate the power generated from PV. A bidirectional boost converter is always used to link the SC to the DC bus; this setup enables the SC to be charged or discharged [27]. In addition, to ensure safe operation and soft dynamics, the current regulation loop regulates all converters. SC control loops are designed to operate substantially more quickly than regular control loops. The EMS produces the i_{FC-REF} and i_{SC-REF} signals. The advantages of this method are focused on controlling the energy of the system stockers, namely the energy of the DC bus and SCs, to determine the best FC power correction effort.

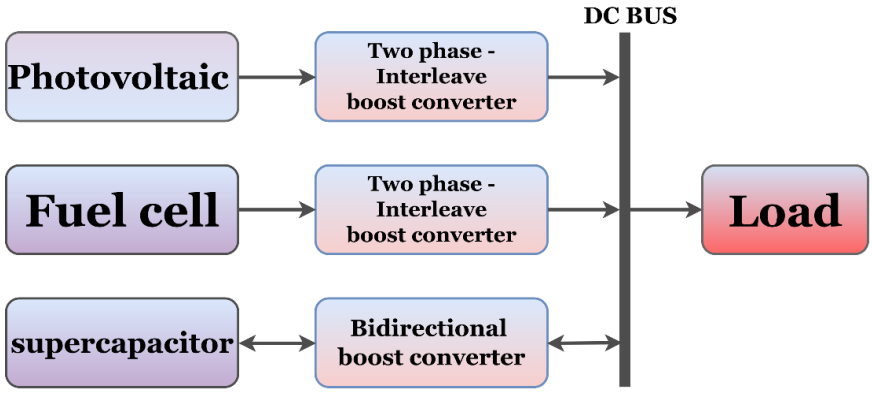

Fig. 1. Proposed system structure

3.1.1. Modelling of PV

The PV system, which uses the PV effect to convert sunlight directly into electricity, is the most well-known type of solar energy. The total PV voltage is increased when PV cells are joined in series to form a module. Then, to increase electrical output, numerous modules are connected in parallel [28]. This increases the total PV current where equation (1) is used to calculate the photocurrent, sometimes referred to as short circuit current, can be describe as [29].

$$I_{sc} = \frac{G}{1000}\left[I_{scr} + k_i(T_c - T_{ref})\right] \quad (1)$$

Where G is the solar irradiation, I_{scr} is the reverse saturation current, k_i is the temperature coefficient, T_c is the cell temperature, T_{ref} is the refrence temperature, Equation (2) is used to determine the open circuit voltage produced at the output of the single-diode solar photovoltaic cell model:

$$V_{oc} = ln\left(\frac{I_{sc}}{I_o} + 1\right)\left(\frac{nkT_c}{q}\right) \quad (2)$$

Where V_{oc} is the open circuit voltage, I_{sc} is the photocurrent,n the ideality factor, I_o the saturation current, k is the Boltzman constant, T_c is the cell temperature, q is the electron charge.

Equation (3) shows the relationship between the solar cell's voltage and current

$$I = I_s\left[exp\left(\frac{qV}{KT}\right) - 1\right] - I_{ph} \quad (3)$$

Where I_s is the saturation current , V is the diode voltage , I_{ph} is the light generated current , T is the ambient temperature.

The main factors that affect a Photovoltaic system's output power are temperature and solar irradiation. As a result, as the temperature of the PV system increases, the voltage falls, which has an impact on the PV system [30]. According to the P-V and I-V features demonstrated in Fig. 2 [31]. The maximum power point tracking (MPPT) technique extracts the power from its maximum point. This figure obviously shows that an operating point (V_{mpp}–I_{mpp})appears as the maximum power obtained from the PV. A DC-DC converter adjusted by the MPPT technique is used to attain this point. This paper uses a modified incremental conductance technique (MINC) [32].

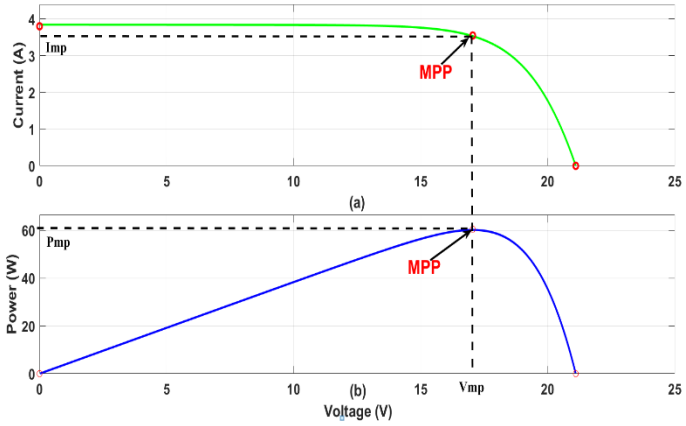

Fig. 2. I-V and P-V characteristics of the proposed PV module

3.1.2. Modelling *of FC*

The polymer membrane is placed in the modeled PEM FC between the two electrodes. As shown in Fig. 3 [33], each comprises a bipolar plate, a channel that allows reactants to flow, a GDL, and a catalyst layer. When oxygen from the cathode and hydrogen from the anode combine, heat and water vapor is created. Forced and natural cooling are used to remove the heat produced by the FC. The power for the load is provided by electrons flowing from the anode toward the cathode. To create a stack and raise the output voltage, many cells are frequently connected in series [34].

$$\textit{Anode:} \quad 2H_2 \rightarrow 4H + 4e^- \tag{4}$$

$$\textit{Cathode:}\ O_2 + 4H + 4e^- \rightarrow 2H_2O \tag{5}$$

$$\textit{Overall:}\ 2H_2 + O_2 \rightarrow 2H_2O \tag{6}$$

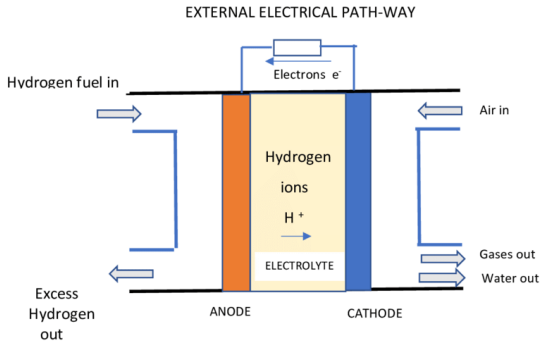

Fig. 3. Schematic diagram of PEMFC

As seen, the output voltage of a one FC cell V_{FC} can be expressed as[34] . These terms can be defined at no-load state as following where electrical model of FC is illustrate in Fig. 4 [35]:

$$V_{FC} = E_{Nernst} - V_{con} - V_{ohmic} - V_{act} \tag{7}$$

E_{Nernst}Where Nernst voltage is the cell's thermodynamic potential, representing its reversible voltage; the Nernst voltage is calculated starting from a modified version of the Nernst equation measured in (V).

$$E_{Nernst} = 1.229 - 0.85 \times 10^{-3}.(T - 298.15) + 4.31 \times 10^{-5}.T[ln(P_{H2}) + 0.5\ ln(P_{O2})\ ] \tag{8}$$

V_{act} the voltage loss measured in (V) during the reaction is known as the activation voltage drop.

$$V_{act} = -[\delta_1 + \delta_2\ .T + \delta_3\ .T.ln(co2) + \delta_4\ .T.ln(i_{FC})] \tag{9}$$

$$co2 = \frac{P_{O2}}{5.08 \times 10^6 \times e^{-\left(\frac{498}{T}\right)}} \tag{10}$$

V_{con}: -is the drop voltage that is produced from the decrease in the concentration of oxygen and hydrogen.

$$V_{con} = -B.ln\left(1 - \frac{J}{J_{max}}\right) \quad (11)$$

V_{ohmic}:-is the ohmic voltage drop that represents voltage loss because of resistance ions flowing in the polymer membrane and resistance to electrons flowing in the electrodes.

$$V_{ohmic} = i_{FC}.(R_m + R_c) \quad (12)$$

The terms of the above s can be defined as:

- T is the FC cell's temperature in (Kelvin).
- P_{H2} is the hydrogen partial pressure in (atmospheres (atm)).
- P_{O2} is the oxygen partial pressure in (atmospheres (atm)).
- B is the cell type constant in the operation state (V).
- J is the current density(A/cm^2).
- J_{max} is the peak value of the current density.
- i_{FC} is the output current of FC (A).
- R_m is the membrane's resistance to proton conduction (Ω).
- R_c is the contact's impedance to electron flow (Ω).
- δ_i $(1 \dots \dots .4)$ defines the FC coefficients.
- co2 is the oxygen concentration in the cathode interface in $molar/cm$

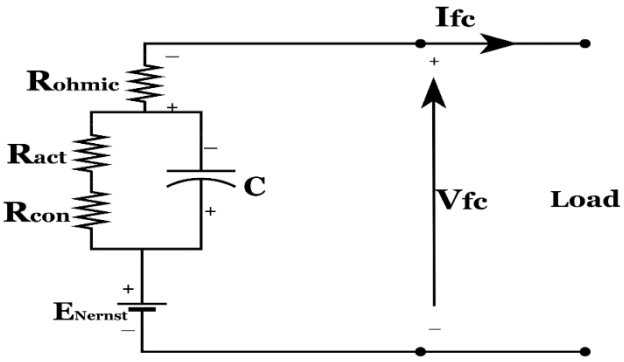

Fig. 4. Electrical Model of FC

3.1.3. SC Modelling

SCs are high-capacity capacitor used in applications that require rapid charges and discharge cycles rather than long-term compact energy storage. It is used for regenerative braking and short-term energy storage [36]. The SC device operates and stores the required electrical energy without a chemical process, making the response time very small. Today, different technologies for SC are available on the market, ranging from 5 to 2700 f, rated at 2.5 Vdc per cell [37] . As presented, the energy storage for each cell is about three, or 4Wh/kg. To increase the output voltage of the SC, more cells must be connected in series to give about 48V for DC applications.

Using SC in MG is very important to control the DC bus voltage and provide the transient power demand or nonlinear load that protects the power electronics equipment. As a result, the SC device can quickly absorb or release voltage. However, MathWorks provided a new version of Simulink (2020) that includes an SC model that allows one to quickly show the SC model with its parameters [38] . Therefore, in this paper, the SC model is derivate form MATLAB/Sim power systems toolbox as seen in Fig. 5.

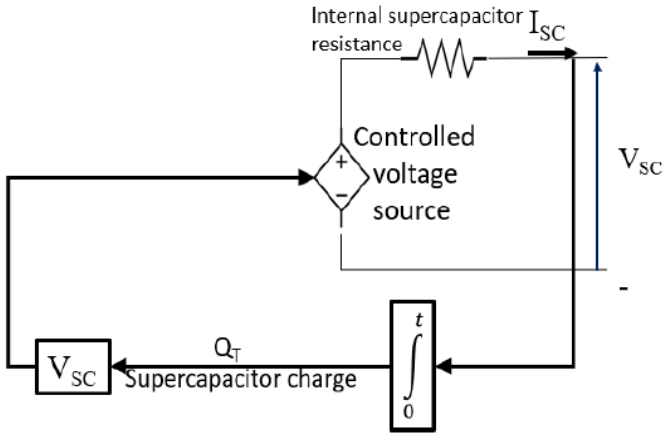

Fig. 5. Electrical Model of SC

3.1.4. Load Modelling

It is suggested to use a dynamic load profile where the necessary power behaves as a controlled current source in this MG, and the load power is equal to:

$$P_{load} = V_{bus}\, i_{load} \tag{13}$$

3.2. Modified INC

The MPPT techniques depend on the traditional INC technique, in which the controller measures incremental changes in V and I of the PV to prophesy the effect of the command; this technique requires additional computations and can track variable conditions more quickly than the P&O technique. This algorithm, regarding the change in step size of the duty cycle at a steady state, results in oscillations in the PV output power, such as the P&O algorithm. A large step size leads to high oscillation. In addition, low-duty cycle variation leads to low oscillations, resulting in slow operation. Therefore, when using a fixed step size, there will be a problem between steady-state oscillation and fast response. A modified variable step size is used to enhance the performance of the MPPT technique, which depends only on the change in PV power change (ΔP):

$$Offset = Offset_1\, abs(\Delta P) \tag{14}$$

Offset1 is the scaling factor adjusted to compromise the response time and reduce steady-state oscillations. The variable in the PV array increases or decreases while the operational point moves toward the MPP. As a result, the operating point moves in and out of the MPP. The flow chart in Fig. 6 lists the primary steps.

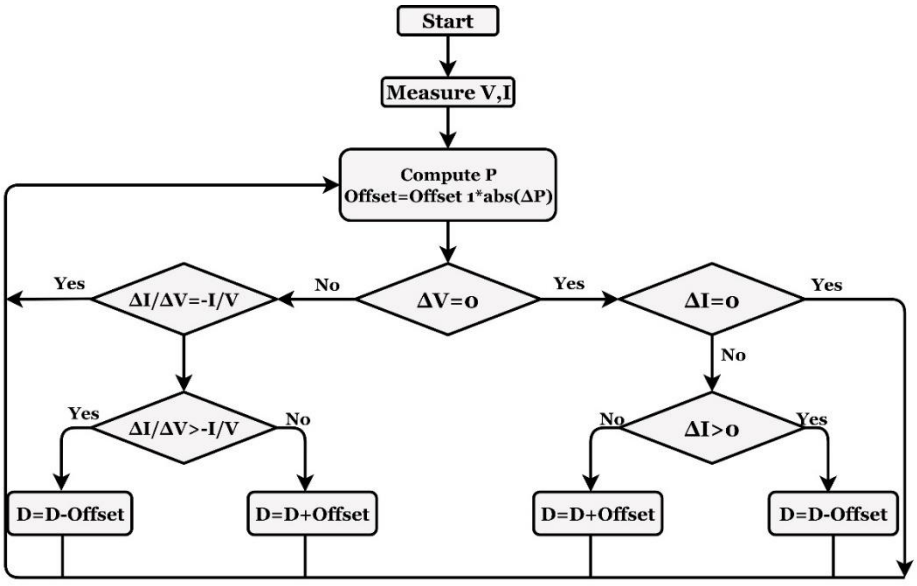

Fig. 6. MINC flow chart

3.3. Modelling of system behaviours

The management system's purpose is to sustain reference of the DC bus voltage value (380 V), where the rapid response of the SC in the cases of charging and discharging achieves this. Therefore, the capacitive energy equations for the DC bus and SC are written as [39].

$$y_{bus} = \frac{1}{2} C_{bus}\, V_{bus}^2 \tag{15}$$

$$y_{sc} = \frac{1}{2} C_{sc}\, V_{sc}^2 \tag{16}$$

$$y_T = y_{bus} + y_{sc} \tag{17}$$

According to Fig. 1, the differential equation will describe the DC-bus capacitive energy, which is written as

$$\dot{y_{bus}} = P_{PVo} + P_{FCo} + P_{SCo} - P_{load} \tag{18}$$

Here, the output powers from each source can be described as P_{PVo}, P_{FCo}, and P_{SCo}severally, including static losses r_{PV}, r_{FC} and r_{SC} for PV, FC, and SC respectively for each converter

$$P_{PVo} = P_{PV} - r_{PV}\left(\frac{P_{PV}}{v_{PV}}\right)^2 \tag{19}$$

$$P_{FCo} = P_{FC} - r_{FC}\left(\frac{P_{FC}}{v_{FC}}\right)^2 \quad (20)$$

$$P_{SCo} = P_{SC} - r_{SC}\left(\frac{P_{SC}}{v_{SC}}\right)^2 \quad (21)$$

Imposing that the power of FC and SC follow their reference values, which are written as

$$P_{FC\_ref} = P_{FC} = v_{FC} i_{FC} \quad (22)$$

$$P_{SC\_ref} = P_{SC} = v_{SC} i_{SC} \quad (23)$$

Also, the load-power equation is

$$P_{load} = i_{load}\, v_{bus} = \sqrt{\frac{2\, y_{bus}}{C_{bus}}}\; i_{load} \quad (24)$$

3.4. Control approach

In this islanded MG, the PV and FC sources must be able to supply the load demand in different cases and charge the SC storage unit. In addition, the PV panel works at MPPT; the MINC technique is depicted in Fig. 6 to achieve more stability in the system. The net power produced may be expressed as follows:

$$P_{Gen} = P_{PVo} + P_{FCo} \quad (25)$$

By substituting in (18) it will be

$$\dot{y_{bus}} = P_{Gen} + P_{SCo} - P_{load} \quad (26)$$

While PV delivers all available power to the load, the FC stack provides the energy needed to compensate for the shortfall. From Equation (25) the generated power can be written as

$$P_{Gen} = \dot{y_{bus}} + P_{load} - P_{sco} \quad (27)$$

3.4.1. Nonlinear flatness control and DC bus voltage control

The entire system's power output is non-linear, which adds complexity to the system. Therefore, applying a differential flatness approach is implemented to convert the system to a linear and reduced-order model, which adds flexibility to the system. These alternative models allow for the description of trajectories that contain their dynamics that concept of differential flatness illustrates in Fig. 7. The system considered flat according to [40, 41] must be expressed as

$$y = \phi\left(x, u, \dot{u}, \ldots\ldots u^{(\alpha)}\right) \quad (28)$$

$$x = \varphi\left(y, \dot{y}, \ldots\ldots y^{(\beta)}\right) \quad (29)$$

$$u = \psi\left(y, \dot{y}, \ldots\ldots y^{(\beta+1)}\right) \quad (30)$$

where y is the output flat model, x is the state variable, and u is the control variable. Also, ϕ, φ, and ψ are smooth mapping the functions, while $y^{(\beta+1)}$ is the notation derivative of the output $(\beta+1)^{\text{th}}$ in addition, α is the finite derivative number of, whilst $rank(\phi) = m, rank(\varphi) = n$, and $rank(\psi) = m$.

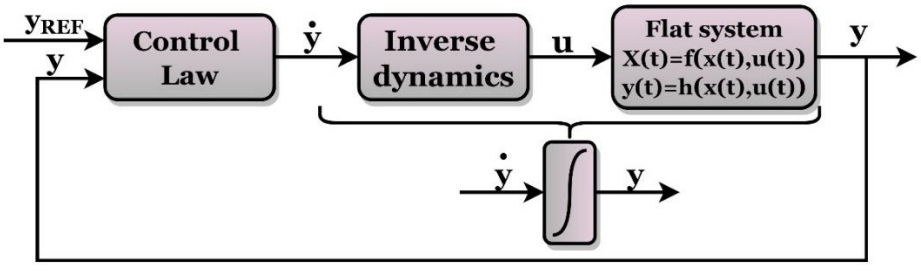

Fig. 7. Structure of differential flatness-based control

Depending on the initial analysis results, the SC supplies the demand load with the fastest available energy to achieve DC bus stability when operating under various conditions. The suggested power system is subjected to flatness control to reduce the model's order and display the suggested management system. The proposed model will be defined by what was discussed in the preceding section according to flies [33]: -

The flat output $\boldsymbol{y} = [y_1\ y_2]^T = [y_{bus}\ \ y_T]^T$
The control variable $u = [u_1\ u_2]^T = [P_{SC}^{ref}\ \ P_{FC}^{ref}]^T$
and the state variable $X = [x_1\ x_2]^T = [V_{bus}\ \ V_{sc}]^T$
From Eqs. (15,16) $V_{bus} = X_1$ and $V_{sc} = X_2$ must be expressed as respectively

$$X_1 = \sqrt{\frac{2y_1}{C_{bus}}} \tag{31}$$

$$X_2 = \sqrt{\frac{2(y_2 - y_1)}{C_{sc}}} \tag{32}$$

From equations (15,17,1 8and 19), the control variable u_1 represent the reference power of SC can be expressed as

$$u_1 = P_{SC,ref} = 2P_{SC,max}\left[1 - \sqrt{1 - \frac{\dot{y}_1 + \sqrt{\frac{2y_1}{C_{bus}}} \cdot i_{load} - (P_{Bo} + P_{FCo} + P_{PVo})}{P_{SC,max}}}\right] \tag{33}$$

Define $P_{SC,max} = \frac{v_{SC}^2}{4\, r_{SC}}$ the SC maximum limited power.

From equations (15,17,18,2 3and 26) the control variable u_2 represent the reference power of FC can be expressed as

$$u_2 = P_{FC,ref} = 2P_{Gen}\left[\sqrt{1 - \sqrt{1 - \frac{\dot{y}_2 + \sqrt{\frac{2y_1}{C_{bus}}} \cdot i_{load}}{P_{G\,max}}}}\right] - P_{PVo} \tag{34}$$

The maximum power generated by the PV and FC converters is known as $P_{G\,max}$

$$P_{G\,max} = P_{FC\,max} + P_{PV\,max} \tag{35}$$

3.4.2. Stabilization of DC bus voltage

A PI classical control law is used to guarantee the control of this flat variable. The DC bus power is given in Eq. (18), assuming that the SC control loop is significantly faster than the FC and PV control loops, which can be roughly represented as

$$\dot{y}_{bus} = P_{SCo} \tag{36}$$

Depending on[42] the DC bus energy is regulated by a PI controller

$$\dot{y}_{bus} = \frac{1}{s}\left(K_p + \frac{K_i}{s}\right)(y_1 - y_{1,ref}) \tag{37}$$

$K_p = 2\,\zeta\omega_n$, $K_i = {\omega_n}^2$. Fig. 8a shows the control structure of DC bus energy.

Where $\omega_n the\ natural\ frequency$, $\zeta\ the\ damping\ factor$.

Also, the PI controller in Fig.8b was used to provide the SC's demand power, which is given as a reference power item to the FC and PV in the following way:

$$P_{SCdem} = K_1(v_{SC,ref} - v_{SC}) + K_2\int(v_{SC,ref} - v_{SC}) \tag{38}$$

where $v_{SC,ref}$ represent the SC's reference voltage, $K_1$is the proportional gain of the charge controller, and K_2 is the integral gain.

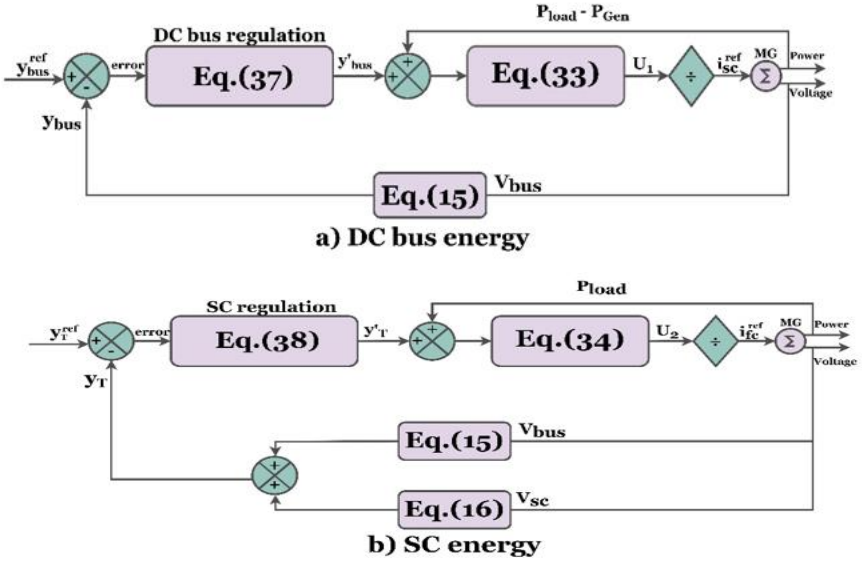

Fig. 8. A control scheme of the proposed work; a) DC bus energy, b) SC energy

4. Results and Discussion

The simulation of the proposed islanded DC microgrid shall validate the performance of the proposed EMS. All sources are linked to a common DC bus, and the control system is used to maintain the voltage at its reference. After the control scheme, the simulation of the hybrid power system was performed in MATLAB/Simulink. To simulate the real-world environment, the demand will vary to maintain the DC bus reference voltage at 380 V in two cases. A power electronic converter connects the sources and the DC bus.

4.1. Case I: change in irradiance and load variation

Solar irradiance changed from 200–600–1000 $^{w}/_{m^2}$, as shown in Fig. 9a, with a change in controllable load. Fig. 9b shows the voltage stability of the DC bus despite several disturbances, where the fast response of the SC will control the DC bus and power balance between sources and load is achieved, as demonstrated in Fig. 9c. At the beginning of running, the SC is discharged utill both PV and FC can cover the power supply to the load as a result of the minimization of irradiance and chemical reaction, respectively. At time = 1.5 seconds, the PV supplies the power to load and the SC starts charging. Fig. 9d displays the SoC of the SC illustrates at which time the SC operates in discharge or charge mode.

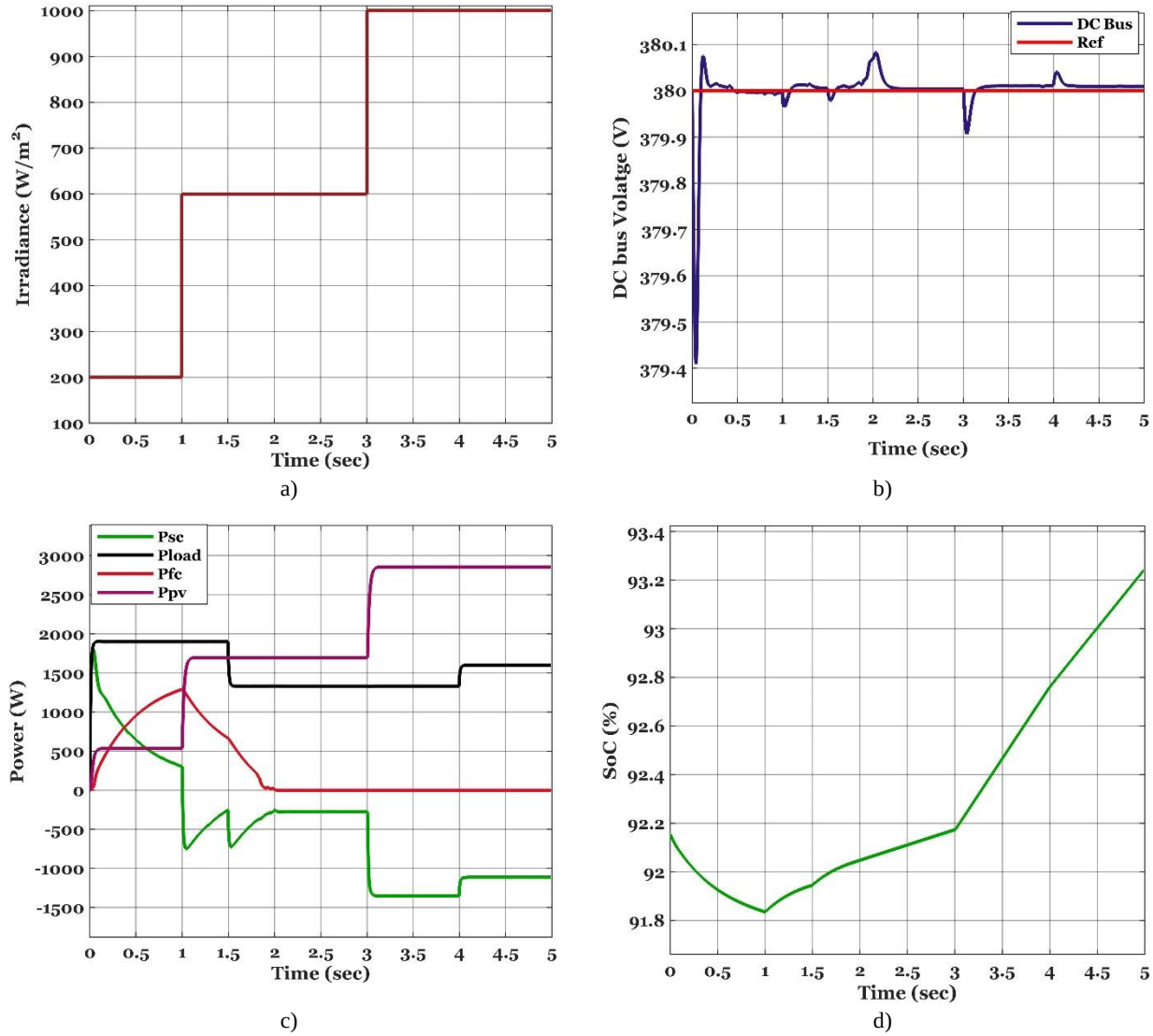

Fig. 9. Case I; a) solar irradiance profile, b) DC bus voltage, c) Powers of PV, FC, SC and load, d) SOC of SC

4.2. Case II: change in irradiance and constant load

Fig. 10a presents the change in solar irradiance change from 400-700-1000 w/m^2, the powers of (SC, PV, and FC) are shared between them to supply the load. At time = 1 sec, the PV's power was increased to 2500 watts, but it could still not supply the load. Therefore, the FC's power decreased to the allowable limit capable of supplying the load as a result of this increase in the PV's power. Additionally, because of the rapid transition in radiation from 400 to 700, as clarified in Fig. 10b, the SC charges this excess power for an instantaneous period. The dynamic behaviour of the SC and the fast transition from charge to discharge is clarified in Fig. 10c. The DC bus voltage stability is enhanced, as illustrated in Fig. 10d.

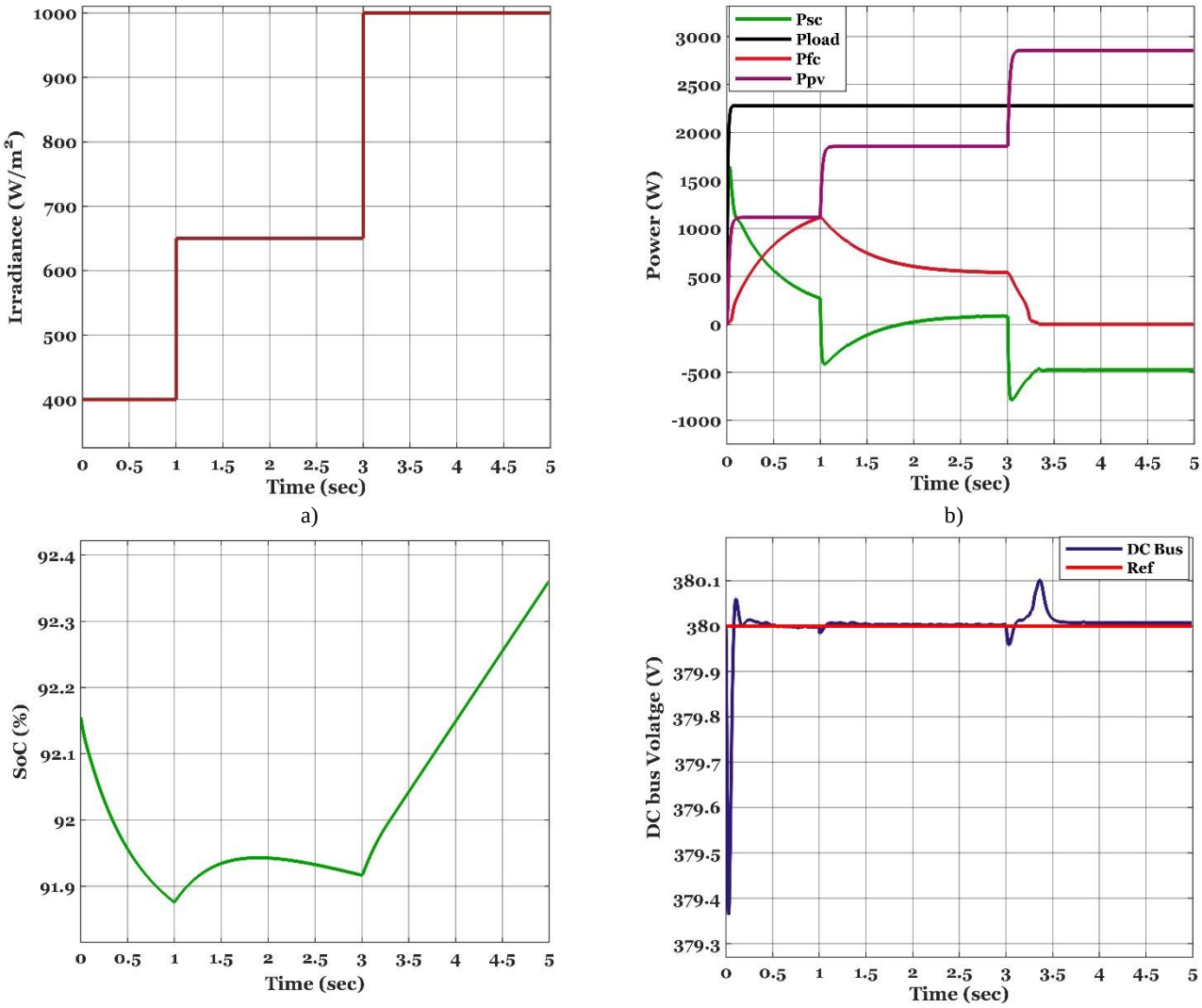

Fig. 10. Case II; a) solar irradiance profile, b) DC bus voltage, c) Powers of PV, FC, SC and load, d) SOC of SC

The utilized of hybrid renewable sources and energy storage shows ability of system continues energy supplying to the load for with different load level and sun irradiance by power sharing between sources. The SC increase system dynamism due to its characteristics. Table 1 illustrates the parameters of the MG. The flatness property has been implemented in a simple nonlinear control approach to solve the problems of dynamics, optimization, stabilization, and robustness of a nonlinear power electronic system. When comparison the ripple in the DC bus voltage and time response with this study[43] , the proposed method offers less ripple in the DC bus voltage and faster time response as demonstrated in Table 2.

Table 1. values of the control system

Parameter	Value
C_{SC}	$120\ F$
C_{bus}	$100\ e^{-5}\ F$
K_1	2
K_2	150
K_p	2000
K_i	70
r_{PV}	0.01
r_{FC}	0.13
r_{SC}	0.08

Table 2. comparison results of flatness-based control and PI controller

load power	Conventional PI		Proposed flatness method	
(W)	Ripple in V_{bus}(V)	Time response (ms)	Ripple in V_{bus}(V)	Time response (ms)
1500	9.5	0.045	7.8	0.03
2500	7.8	0.04	6.3	0.039
3000	8.7	0.05	6.65	0.052

5. Conclusion

The main contribution of this work is to present an efficient energy management strategy for a hybrid power plant composed of PV, FC, and SC. This strategy is suitable for high-power applications. The design procedure, working principle, and analysis are discussed. PV and FC are essential sources, where FC acts as a support source to fill the steady state of the shortage that occurs in the solar panel. In contrast, the supercapacitor tasks as a storage source to compensate for the PV and FC sources' luck in the transient and steady states. The differential flatness approach determines how to use non-linear control also performs better than classical PI controllers in terms of stability and optimum response to the 380 V dc-bus voltage regulation. This study proposed a power sharing between different sources under variable operating conditions, which is suitable for stabilisation and robustness problems. Furthermore, the mathematical model of the hybrid power plant accurately predicts the system's dynamics.

The study is recommended for future work:1) Connecting an inverter after the DC bus to supply critical loads in the event of a fault in the main grid, and 2) Implementation of an EMS for the smart grid based on the optimization approach.

Acknowledgment

The authors would like to thank all the College of Electrical and Electronic Technology staff for their unlimited support in completing this study.

References

[1] M. S. Răboacă et al., "Concentrating solar power technologies," Energies, vol. 12, no. 6, p. 1048, 2019.
[2] K. Lovegrove and W. Stein, "Concentrating solar power technology: principles, developments and applications," 2012.
[3] B. P. Singh, S. K. Goyal, and S. A. Siddiqui, "Grid connected-photovoltaic system (GC-PVS): Issues and challenges," in IOP Conference Series: Materials Science and Engineering, 2019, vol. 594, no. 1: IOP Publishing, p. 012032.
[4] D. Akinyele, E. Olabode, and A. Amole, "Review of fuel cell technologies and applications for sustainable microgrid systems," Inventions, vol. 5, no. 3, p. 42, 2020.
[5] M. H. Rahman, K. Barua, M. Anis-Uz-Zaman, M. A. Razak, and N. Islam, "Simulation of a solar power system with fuel cell backup source for hybrid power system application," in 2019 International Conference on Energy and Power Engineering (ICEPE), 2019: IEEE, pp. 1-4.
[6] P. Thounthong and S. Rael, "The benefits of hybridization," IEEE Industrial Electronics Magazine, vol. 3, no. 3, pp. 25-37, 2009.
[7] W. Jing, C. H. Lai, W. S. Wong, and M. D. Wong, "A comprehensive study of battery-supercapacitor hybrid energy storage system for standalone PV power system in rural electrification," Applied energy, vol. 224, pp. 340-356, 2018.
[8] C. Wang and M. H. Nehrir, "Power management of a stand-alone wind/photovoltaic/fuel cell energy system," IEEE transactions on energy conversion, vol. 23, no. 3, pp. 957-967, 2008.
[9] S. A. Shezan et al., "Performance analysis of an off-grid wind-PV (photovoltaic)-diesel-battery hybrid energy system feasible for remote areas," Journal of Cleaner Production, vol. 125, pp. 121-132, 2016.
[10] J. Lian, Y. Zhang, C. Ma, Y. Yang, and E. Chaima, "A review on recent sizing methodologies of hybrid renewable energy systems," Energy Conversion and Management, vol. 199, p. 112027, 2019.
[11] M. Dahmane, J. Bosche, and A. El-Hajjaji, "Power management strategy for renewable hybrid stand-alone power system," in 2015 4th International Conference on Systems and Control (ICSC), 2015: IEEE, pp. 247-254.
[12] T. Castillo-Calzadilla, C. M. Andonegui, M. Gómez-Goiri, A. M. Macarulla, and C. E. Borges, "Systematic analysis and design of water networks with solar photovoltaic energy," IEEE Transactions on Engineering Management, 2019.
[13] O. O. Mengi and I. H. Altas, "A fuzzy decision making energy management system for a PV/Wind renewable energy system," in 2011 International Symposium on Innovations in Intelligent Systems and Applications, 2011: IEEE, pp. 436-440.
[14] H. Kakigano, Y. Miura, T. Ise, and R. Uchida, "DC micro-grid for super high quality distribution—System configuration and control of distributed generations and energy storage devices," in 2006 37th IEEE Power Electronics Specialists Conference, 2006: IEEE, pp. 1-7.
[15] A. A. Gonzalez, M. Bottarini, I. Vechiu, L. Gautier, L. Ollivier, and L. Larre, "Model Predictive Control for the Energy Management of A Hybrid PV/Battery/Fuel Cell Power Plant," in 2019 International Conference on Smart Energy Systems and Technologies (SEST), 2019: IEEE, pp. 1-6.
[16] A. M. Al-Antaki, T. Golubchik, M. A. Al-Furaiji, and H. Mohammed, "Control of hybrid DC/AC microgrid system employing fuel cell and solar photovoltaic sources using grey wolf optimization," Clean Energy, vol. 6, no. 4, pp. 659-670, 2022.
[17] V. Vinod and A. Singh, "A comparative analysis of PID and fuzzy logic controller in an autonomous PV-FC microgrid," in 2018 International Conference on Control, Power, Communication and Computing Technologies (ICCPCCT), 2018: IEEE, pp. 381-385.
[18] P. Singh and J. S. Lather, "Variable structure control for dynamic power-sharing and voltage regulation of DC microgrid with a hybrid energy storage system," International Transactions on Electrical Energy Systems, vol. 30, no. 9, p. e12510, 2020.
[19] S. Sinha and P. Bajpai, "Power management of hybrid energy storage system in a standalone DC microgrid," Journal of Energy Storage, vol. 30, p. 101523, 2020.
[20] H. Marzougui, A. Kadri, J.-P. Martin, M. Amari, S. Pierfederici, and F. Bacha, "Implementation of energy management strategy of hybrid power source for electrical vehicle," Energy Conversion and Management, vol. 195, pp. 830-843, 2019.
[21] M. A. Danzer, J. Wilhelm, H. Aschemann, and E. P. Hofer, "Model-based control of cathode pressure and oxygen excess ratio of a PEM fuel cell system," Journal of Power Sources, vol. 176, no. 2, pp. 515-522, 2008.
[22] E. Song, A. F. Lynch, and V. Dinavahi, "Experimental validation of nonlinear control for a voltage source converter," IEEE Transactions on Control Systems Technology, vol. 17, no. 5, pp. 1135-1144, 2009.
[23] A. Gensior, H. Sira-Ramírez, J. Rudolph, and H. Guldner, "On some nonlinear current controllers for three-phase boost rectifiers," IEEE transactions on industrial electronics, vol. 56, no. 2, pp. 360-370, 2008.
[24] S. K. Agrawal, K. Pathak, J. Franch, R. Lampariello, and G. Hirzinger, "A differentially flat open-chain space robot with arbitrarily oriented

joint axes and two momentum wheels at the base," IEEE Transactions on Automatic Control, vol. 54, no. 9, pp. 2185-2191, 2009.
[25] M. Lazić, M. Živanov, and B. Šašić, "Desing of multiphase boost converter for hybrid fuel cell/battery power sources," Paths to Sustainable Energy, INTECH 2010, pp. 359-404, 2010.
[26] P. Prasanth and R. Seyezhai, "Investigation of four phase interleaved boost converter under open loop and closed loop control schemes for battery charging applications," Int. J. Adv. Mater. Sci. Eng, vol. 5, no. 1, pp. 11-20, 2016.
[27] S. Jadhav, N. Devdas, S. Nisar, and V. Bajpai, "Bidirectional DC-DC converter in solar PV system for battery charging application," in 2018 International Conference on Smart City and Emerging Technology (ICSCET), 2018: IEEE, pp. 1-4.
[28] A. J. Abid, A. Obed, and F. M. Al-Naima, "Detection and control of power loss due to soiling and faults in photovoltaic solar farms via wireless sensor network," International Journal of Engineering & Technology, vol. 7, no. 2, pp. 718-724, 2018.
[29] M. Kamran, M. Mudassar, M. R. Fazal, M. U. Asghar, M. Bilal, and R. Asghar, "Implementation of improved Perturb & Observe MPPT technique with confined search space for standalone photovoltaic system," Journal of King Saud University-Engineering Sciences, vol. 32, no. 7, pp. 432-441, 2020.
[30] A. M. Humada, M. Hojabri, S. Mekhilef, and H. M. Hamada, "Solar cell parameters extraction based on single and double-diode models: A review," Renewable and Sustainable Energy Reviews, vol. 56, pp. 494-509, 2016.
[31] S. Motahhir, A. Chalh, A. El Ghzizal, S. Sebti, and A. Derouich, "Modeling of photovoltaic panel by using proteus," Journal of Engineering Science and Technology Review, vol. 10, pp. 8-13, 2017.
[32] S. Motahhir, A. El Ghzizal, S. Sebti, and A. Derouich, "MIL and SIL and PIL tests for MPPT algorithm," Cogent Engineering, vol. 4, no. 1, p. 1378475, 2017.
[33] D. Murray-Smith, "A Review of Developments in Electrical Battery, Fuel Cell and Energy Recovery Systems for Railway Applications: a Report for the Scottish Association for Public Transport," 2019.
[34] J. M. Correa, F. A. Farret, V. A. Popov, and M. G. Simoes, "Sensitivity analysis of the modeling parameters used in simulation of proton exchange membrane fuel cells," IEEE Transactions on energy conversion, vol. 20, no. 1, pp. 211-218, 2005.
[35] A. S. Samosir, T. Sutikno, and A. H. M. Yatim, "Dynamic evolution control for fuel cell DC-DC converter," TELKOMNIKA (Telecommunication Computing Electronics and Control), vol. 9, no. 1, pp. 183-190, 2011.
[36] Y. Li, J. Song, and J. Yang, "A review on structure model and energy system design of lithium-ion battery in renewable energy vehicle," Renewable and Sustainable Energy Reviews, vol. 37, pp. 627-633, 2014.
[37] S. O. Amrouche, D. Rekioua, T. Rekioua, and S. Bacha, "Overview of energy storage in renewable energy systems," International journal of hydrogen energy, vol. 41, no. 45, pp. 20914-20927, 2016.
[38] S. Ferahtia et al., "Optimal adaptive gain LQR-based energy management strategy for battery–supercapacitor hybrid power system," Energies, vol. 14, no. 6, p. 1660, 2021.
[39] P. Thounthong, P. Tricoli, and B. Davat, "Performance investigation of linear and nonlinear controls for a fuel cell/supercapacitor hybrid power plant," International Journal of Electrical Power & Energy Systems, vol. 54, pp. 454-464, 2014.
[40] M. Fliess, J. Lévine, P. Martin, F. Ollivier, and P. Rouchon, "Controlling nonlinear systems by flatness," in Systems and Control in the Twenty-first Century: Springer, 1997, pp. 137-154.
[41] L. Maheswari and N. Sivakumaran, "Differential flatness-based strategy of Photovoltaic/Battery/supercapacitor hybrid source for stand-alone system," Materials Today: Proceedings, vol. 46, pp. 10036-10042, 2021.
[42] A. L. S. Budi, S. Anam, M. Ashari, and A. Soeprijanto, "Energy Management Control Based on Standalone Photovoltaic Battery and Supercapacitor Hybrid Energy Storage System Using PI Controller," in International Seminar of Science and Applied Technology (ISSAT 2020), 2020: Atlantis Press, pp. 1-7.
[43] S. K. Ghosh, T. K. Roy, M. A. H. Pramanik, A. K. Sarkar, and M. A. Mahmud, "An energy management system-based control strategy for DC microgrids with dual energy storage systems," Energies, vol. 13, no. 11, p. 2992, 2020.